Shift in the velocity of a front due to a cut-off

Eric BRUNET and Bernard DERRIDA

Laboratoire de Physique Statistique, ENS, 24 rue Lhomond, 75005 Paris, France

Abstract

We consider the effect of a small cut-off ε on the velocity of a traveling wave in one dimension. Simulations done over more than ten orders of magnitude as well as a simple theoretical argument indicate that the effect of the cut-off ε is to select a single velocity which converges when $\varepsilon \to 0$ to the one predicted by the marginal stability argument. For small ε, the shift in velocity has the form $K(\log \varepsilon)^{-2}$ and our prediction for the constant K agrees very well with the results of our simulations. A very similar logarithmic shift appears in more complicated situations, in particular in finite size effects of some microscopic stochastic systems. Our theoretical approach can also be extended to give a simple way of deriving the shift in position due to initial conditions in the Fisher-Kolmogorov or similar equations.

PACS: 02.50.Ey, 03.40.Kf, 47.20.Ky

1 Introduction

Equations describing the propagation of a front between a stable and an unstable state appear [1, 2, 3, 4, 5, 6, 7] in a large variety of situations in physics, chemistry and biology. One of the simplest equations of this kind is the Fisher-Kolmogorov [1, 2] equation

$$\frac{\partial h}{\partial t} = \frac{\partial^2 h}{\partial x^2} + h - h^3, \qquad (1)$$

which describes the evolution of a space and time dependent concentration $h(x,t)$ in a reaction-diffusion system. This equation, originally introduced to study the spread of advantageous genes in a population [1], has been widely used in other contexts, in particular to describe the time dependence of the concentration of some species in a chemical reaction [8, 9].

For such an equation, the uniform solutions $h = 1$ and $h = 0$ are respectively stable and unstable and it is known [3, 7, 10, 11, 12] that for initial conditions such that $h(x,0) \to 1$ as $x \to -\infty$ and $h(x,0) \to 0$ as $x \to +\infty$ there exists a one parameter family F_v of traveling wave solutions (indexed by their velocity v)

of the form

$$h(x,t) = F_v(x - vt), \qquad (2)$$

with F_v decreasing, $F_v(z) \to 1$ as $z \to -\infty$ and $F_v(z) \to 0$ as $z \to \infty$. The analytic expression of the shape F_v is in general not known but one can determine the range of velocities v for which solutions of type (2) exist. If one assumes an exponential decay

$$F_v(z) \simeq e^{-\gamma z} \qquad \text{for large } z, \qquad (3)$$

it is easy to see by replacing (2) and (3) into (1) that the velocity v is given by

$$v(\gamma) = \gamma + \frac{1}{\gamma}. \qquad (4)$$

As γ is arbitrary, this shows the well known fact that the range of possible velocities is $v \geq 2$. The minimal velocity $v_0 = 2$ is reached for $\gamma_0 = 1$ and for steep enough initial conditions $h(x,0)$ (which decay faster than $e^{-\gamma_0 x}$), the solution selected [3, 4, 6, 7, 10, 11, 12] for large t is the one corresponding to this minimal velocity v_0.

Equations of type (1) are obtained either as the large scale limit [5, 8, 13, 14, 15, 16] or as the mean field limit [17] of physical situations which are discrete at the microscopic level (particles, lattice models, etc.) As the number of particles is an integer, the concentration $h(x,t)$ could be thought as being larger than some ε, which would correspond to the value of $h(x,t)$ when a single particle is present. Equations of type (1) appear then as the limit of the discrete model when $\varepsilon \to 0$. Several authors [8, 13, 14] have already noticed in their numerical works that the speed v_ε of the discrete model converges slowly, as ε tends to 0, towards the minimal velocity v_0. We believe that the main effect of having $\varepsilon \neq 0$ is to introduce a cut-off in the tail of the front, and that this changes noticeably the speed.

The speed of the front is in general governed by its tail. In the present work, we consider equations similar to (1), which we modify in such a way that whenever $h(x,t)$ is much smaller than a cut-off ε, it is replaced by 0. The cut-off ε can be introduced by replacing (1) by

$$\frac{\partial h}{\partial t} = \frac{\partial^2 h}{\partial x^2} + (h - h^3)a(h), \qquad (5)$$

with

$$a(h) = 1 \qquad \text{if } h > \varepsilon, \qquad (6)$$
$$a(h) \ll 1 \qquad \text{if } h \ll \varepsilon.$$

For example, one could choose $a(h) = 1$ for $h \geq \varepsilon$ and $a(h) = h/\varepsilon$ for $h \leq \varepsilon$. Another choice that we will use in section 4 is simply $a(h) = 1$ if $h > \varepsilon$ and $a(h) = 0$ if $h \leq \varepsilon$.

The question we address here is the effect of the cut-off ε on the velocity v_ε of the front. We will show that the velocity v_ε converges, as $\varepsilon \to 0$, to the minimal velocity v_0 of the original problem (without cut-off) and that the main correction to the velocity of the front is

$$v_\varepsilon \simeq v_0 - \frac{\pi^2 \gamma_0^2}{2} \, v''(\gamma_0) \, \frac{1}{(\log \varepsilon)^2} \qquad (7)$$

for an equation of type (1) for which the velocity is related to the exponential decay γ of the shape (2)

by some relation $v(\gamma)$. (Everywhere we note by v_0 the minimal velocity and γ_0 the corresponding value of the decay γ.) In the particular case of equation (1), where $v(\gamma)$ is given by (4), this becomes

$$v_\varepsilon \simeq 2 - \frac{\pi^2}{(\log \varepsilon)^2}. \qquad (8)$$

In section 2 we describe an equation of type (1) where both space and time are discrete, so that simulations are much easier to perform. The results of the numerical simulations of this equation are described in section 3: as $\varepsilon \to 0$, the velocity is seen to converge like $(\log \varepsilon)^{-2}$ to the minimal velocity v_0, and the shape of the front appears to take a scaling form.

In section 4 we show that for equations of type (1) in presence of a small cut-off ε as in (5), one can calculate both the shape of the front and the shift in velocity. The results are in excellent agreement with the numerical data of section 3.

In section 5 we consider a model defined, for a finite number N of particles, by some microscopic stochastic dynamics which reduces to the front equation of sections 3 and 4 in the limit $N \to \infty$. Despite the presence of noise, our simulations indicate that in this case too, the velocity dependence of the front decays slowly (as $(\log N)^{-2}$) to the minimal velocity v_0 of the front.

2   A discrete front equation

To perform numerical simulations, it is much easier to study a case where both time and space are discrete variables. We consider here the equation

$$h(x, t+1) = g(x, t) \, \Theta[g(x, t) - \varepsilon], \qquad (9a)$$

where

$$g(x, t) = 1 - \big[1 - ph(x-1, t) - (1-p)h(x, t)\big]^2. \qquad (9b)$$

Time is a discrete variable and if initially the concentration $h(x, 0)$ is only defined when x is an integer, $h(x, t)$ remains so at any later time. Because t and x are both integers, the cut-off ε can be introduced as

in (9) in the crudest way using a Heaviside Θ function. (We have checked however that other ways of introducing the cut-off ε as in (5, 6) do not change the results.)

Equation (9) appears naturally (in the limit $\varepsilon = 0$) in the problem of directed polymers on disordered trees [17, 18] (where the energy of the bonds is either 1 with probability p or 0 with probability $1-p$). At this stage we will not give a justification for introducing the cut-off ε. This will be discussed in section 5.

We consider for the initial condition a step function

$$
\begin{aligned}
h(x,0) &= 0 && \text{if } x \geq 0, \\
h(x,0) &= 1 && \text{if } x < 0.
\end{aligned}
\tag{10}
$$

Clearly for such an initial condition, $h(x,t) = 1$ for $x < 0$ at all times. As $h(x,t) \simeq 1$ behind the front and $h(x,t) \simeq 0$ ahead of the front, we define the position X_t of the front at time t by

$$
X_t = \sum_{x=0}^{+\infty} h(x,t).
\tag{11}
$$

The velocity of the front v_ε can then be calculated by

$$
v_\varepsilon = \lim_{t \to \infty} \frac{X_t}{t} = \langle X_{t+1} - X_t \rangle,
\tag{12}
$$

where the average is taken over time. (Note that as $h(x,t)$ is only defined on integers, the difference $X_{t+1} - X_t$ is time dependent and has to be averaged as in (12).)

When $\varepsilon = 0$, the evolution equation (9) becomes

$$
h(x,t+1) = 1 - \left[1 - ph(x-1,t) - (1-p)h(x,t)\right]^2.
\tag{13}
$$

As for (1), there is a one parameter family of solutions F_v of the form (2) indexed by the velocity v which is related (3) to the exponential decay γ of the shape by

$$
v(\gamma) = \frac{1}{\gamma} \log\bigl(2pe^\gamma + 2(1-p)\bigr).
\tag{14}
$$

(This relation is obtained as (4) by considering the tail of the front where $h(x,t)$ is small and where therefore (13) can be linearized.)

One can show that for $p < \frac{1}{2}$, $v(\gamma)$ reaches a minimal value v_0 smaller than 1 for some γ_0, whereas for $p \geq \frac{1}{2}$, $v(\gamma)$ is a strictly decreasing function of γ, implying that the minimal velocity is $v_0 = \lim_{\gamma \to \infty} v(\gamma) = 1$.

We will not discuss here this phase transition and we assume from now on that $p < \frac{1}{2}$. Table 1 gives some values of v_0 and γ_0 obtained from (14).

p	0.05	0.25	0.45
γ_0	$2.751111\ldots$	$2.553244\ldots$	$4.051851\ldots$
v_0	$0.451818\ldots$	$0.810710\ldots$	$0.979187\ldots$

Table 1: Values of γ_0 and v_0 for some p when $\varepsilon = 0$.

It is important to notice that for $p < \frac{1}{2}$, the function $v(\gamma)$ has a single minimum at γ_0. Therefore, there are in general two choices γ_1 and γ_2 of γ for each velocity v. For $v \neq v_0$, the exponential decay of $F_v(z)$ is dominated by $\min(\gamma_1, \gamma_2)$. As $v \to v_0$, the two roots γ_1 and γ_2 become equal, and the effect of this degeneracy gives (in a well chosen frame)

$$
F_{v_0}(z) \simeq A z e^{-\gamma_0 z} \qquad \text{for large } z,
\tag{15}
$$

where A is a constant. This large z behavior can be recovered by looking at the general solution of the linearized form of equation (13)

$$
h(x,t+1) = 2ph(x-1,t) + 2(1-p)h(x,t).
\tag{16}
$$

3 Numerical determination of the velocity

We iterated numerically (9) with the initial condition (10) for several choices of $p < \frac{1}{2}$ and for ε varying between 0.03 and 10^{-17}. We observed that the speed is usually very easy to measure because, after a short transient time, the system reaches a periodic regime for which

$$
h(x,t+T) = h(x-Y,t)
\tag{17}
$$

3

for some constants T and Y. The speed v_ε of the front is then simply given by

$$v_\varepsilon = \frac{Y}{T}. \qquad (18)$$

For example, for $p = 0.25$ and $\varepsilon = 10^{-5}$, we find $T = 431$ and $Y = 343$ so that $v_\varepsilon = 343/431$. The emergence of this periodic behavior is due to the locking of the dynamical system of the $h(x,t)$ on a limit cycle. Because Y and T are integers, our numerical simulations give the speed with an *infinite accuracy.*

For each choice of p and ε, we measured the speed of the front, as defined by (12) and its shape. Figure 1 is a log-log plot of the difference $v_0 - v_\varepsilon$ versus ε (varying between 0.03 to 10^{-17}) for three choices of the parameter p. The solid lines on the plot indicate the value predicted by the calculations of section 4.
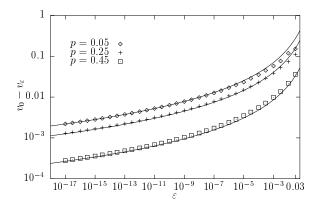

Figure 1: The difference $v_0 - v_\varepsilon$ for $p = 0.05$, 0.25 and 0.5. The symbols represent the result of our numerical simulations and the solid lines indicate the prediction of the analysis of section 4.

We see on this figure that the velocity v_ε converges slowly towards the minimal velocity v_0 as $\varepsilon \to 0$. Our simulations, done over several orders of magnitude (here, fifteen), reveal that the convergence is logarithmic: $v_0 - v_\varepsilon \sim (\log \varepsilon)^{-2}$.

As the front is moving, to measure its shape, we need to locate its position. Here we use expression (11) and we measure the shape $s_\varepsilon(z)$ of the front at a given time t relative to its position X_t by

$$s_\varepsilon(z) = h(z + X_t, t) \qquad (19)$$

When the system reaches the limit cycle (17), the shape $s_\varepsilon(z)$ becomes roughly independent of the time chosen. (In fact it becomes periodic of period T, but the shape s_ε has a smooth envelope.) We have measured this shape at some arbitrary large enough time to avoid transient effects. As we expect $s_\varepsilon(z)$ to look more and more like $F_{v_0}(z)$ as ε tends to 0, we normalize this shape by dividing it by $e^{-\gamma_0 z}$. The result $s_\varepsilon(z)e^{\gamma_0 z}$ is plotted versus z for $p = 0.25$ and $\varepsilon = 10^{-9}$, 10^{-11}, 10^{-13}, 10^{-15} and 10^{-17} in figure 2.
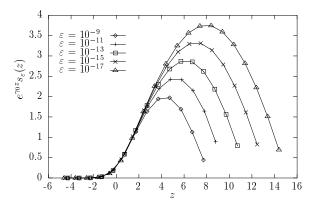

Figure 2: Normalized shape of the front $s_\varepsilon(z)e^{\gamma_0 z}$ versus z for $p = 0.25$ and several choices of ε.

On the left part of the graph, our data coincide over an increasing range as ε decreases, indicating that far from the cut-off, the shape converges to expression (15) of $F_{v_0}(z)$. On the right part, the curves increase up to a maximum before falling down to some small value which seems to be independent of ε. When ε is multiplied by a constant factor (here 10^{-2}), the maximum as well as the right part of the curves are translated by a constant amount. This indicates that for ε small enough, the shape $s_\varepsilon(z)$ in the tail (that is for z large) takes the scaling form

$$s_\varepsilon(z) \simeq |\log \varepsilon| \; G\left(\frac{z}{|\log \varepsilon|}\right) \; e^{-\gamma_0 z}. \qquad (20)$$

4

We will see that our analysis of section 4 does predict this scaling form. As one expects this shape to coincide with the asymptotic form (15) of $F_{v_0}(z)$ for $1 \ll z \ll |\log \varepsilon|$, the scaling function $G(y)$ should be linear for small y.

4 Calculation of the velocity for a small cut-off

The first remark we make is that as soon as we introduce a cut-off through a function $a(h)$ which is everywhere smaller than 1, the velocity v_ε of the front is lowered compared to the velocity obtained in the absence of a cut-off. This is easy to check by comparing a solution $h_\varepsilon(x, t)$ of (5) where $a(h)$ is present and a solution $h_0(x, t)$ of (1). If initially $h_\varepsilon(x, 0) < h_0(x, 0)$, the solution h_ε will never be able to take over the solution h_0. Indeed, would the two functions $h_\varepsilon(x, 0)$ and $h_0(x, 0)$ coincide for the first time at some point x, we would have at that point $\partial^2 h_\varepsilon / \partial x^2 \leq \partial^2 h_0 / \partial x^2$ and together with the effect of $a(h)$ this would bring back the system in the situation where $h_\varepsilon(x, t) < h_0(x, t)$ [3, 7]. This shows that $v_\varepsilon \leq v_0$.

For the calculation of the velocity v_ε, we will consider first the modified Fisher-Kolmogorov equation (5) when the cut-off function $a(h)$ is simply given by

$$a(h) = \Theta(h - \varepsilon). \tag{21}$$

In this section we will calculate the leading correction to the velocity when ε is small and we will obtain the scaling function G which appears in (20). Then we will discuss briefly how our analysis could be extended to more general forms of the cut-off function $a(h)$ or to other traveling wave equations such as (9).

As v_ε is the velocity of the front, its shape $s_\varepsilon(z) = h(z + v_\varepsilon t, t)$ in the asymptotic regime satisfies

$$v_\varepsilon s_\varepsilon' + s_\varepsilon'' + (s_\varepsilon - s_\varepsilon^2) a(s_\varepsilon) = 0.$$

When ε is small, with the choice (21) for $a(h)$, we can decompose the range of values of z into three regions:

Region I where $s_\varepsilon(z)$ is not small compared to 1.

Region II where $\varepsilon < s_\varepsilon(z) \ll 1$.
Region III where $s_\varepsilon(z) < \varepsilon$.

In region I, the shape of the front s_ε looks like F_{v_0} whereas in regions II and III, as s_ε is small, it satisfies the linear equations

$$v_\varepsilon s_\varepsilon' + s_\varepsilon'' + s_\varepsilon = 0 \qquad \text{in region II,} \tag{22}$$
$$v_\varepsilon s_\varepsilon' + s_\varepsilon'' = 0 \qquad \text{in region III.} \tag{23}$$

These linear equations (22,23) can be solved easily. The only problem is to make sure that the solution in region II and its derivative coincides with F_{v_0} at the boundary between I and II and with the solution valid in region III at the boundary between II and III. If we call Δ the shift in the velocity

$$\Delta = v_0 - v_\varepsilon, \tag{24}$$

and if we note $\gamma_r \pm i\gamma_i$ the two roots of the equation $v(\gamma) = v_\varepsilon$, the shape s_ε is given in the three regions by

$$\begin{aligned} s_\varepsilon(z) &\simeq & F_{v_0}(z) & \quad \text{in region I,} \\ s_\varepsilon(z) &\simeq & Ce^{-\gamma_r z} \sin(\gamma_i z + D) & \quad \text{in region II,} \\ s_\varepsilon(z) &\simeq & \varepsilon e^{-v_\varepsilon(z - z_0)} & \quad \text{in region III,} \end{aligned} \tag{25}$$

and we can determine the unknown quantities C, D, z_0 and v_ε by using the boundary conditions.

For large z we know from (15) that $F_{v_0}(z) \simeq Aze^{-\gamma_0 z}$ for some A. Therefore, as $\gamma_0 - \gamma_r \sim \Delta$ and $\gamma_i \sim \Delta^{1/2}$, the boundary conditions between regions I and II impose, to leading order in $\Delta^{1/2}$, that $C = A/\gamma_i$ and $D = 0$.

At the boundary between regions II and III, we have $s_\varepsilon(z) = \varepsilon$ and $z = z_0$. If we impose the continuity of s_ε and of its first derivative at this point, we get

$$Ae^{-\gamma_r z_0} \sin(\gamma_i z_0) = \varepsilon \gamma_i, \tag{26a}$$

and

$$Ae^{-\gamma_r z_0}[-\gamma_r \sin(\gamma_i z_0) + \gamma_i \cos(\gamma_i z_0)] = -v_\varepsilon \varepsilon \gamma_i. \tag{26b}$$

Taking the ratio between these two relations leads to

$$\gamma_r - \frac{\gamma_i}{\tan(\gamma_i z_0)} = v_\varepsilon. \tag{27}$$

When Δ is small, $\gamma_r \simeq \gamma_0 = 1$, $v_\varepsilon \simeq v_0 = 2$ and $\gamma_i \sim \Delta^{1/2}$. Thus the only way to satisfy (27) is to set $\gamma_i z_0 \simeq \pi$ and $\pi - \gamma_i z_0 \simeq \gamma_i \sim \Delta^{1/2}$. Therefore, (26) implies to leading order that $z_0 \simeq -(\log \varepsilon)/\gamma_0$ and the condition $\gamma_i z_0 \simeq \pi$ gives

$$\gamma_i \simeq \frac{\pi}{z_0} \simeq \frac{\pi \gamma_0}{|\log \varepsilon|} \qquad (28)$$

Then, as γ_i is small, the difference $\Delta = v_0 - v_\varepsilon$ is given by

$$v_0 - v_\varepsilon \simeq \frac{1}{2} v''(\gamma_0)\gamma_i^2 \simeq \frac{v''(\gamma_0)\pi^2 \gamma_0^2}{2 (\log \varepsilon)^2} \qquad (29)$$

which is the result announced in (7) and (8).

A different cut-off function $a(h)$ should not affect the shape of s_ε in the region II or the size z_0 of region II. Only the precise matching between regions II and III might be modified and we do not think that this would change the leading dependency of z_0 in ε which controls everything. In fact there are other choices of the cut-off function $a(h)$ (piecewise constant) for which we could find the explicit solution in region III, confirming that the precise form of $a(h)$ does not change (28). The generalization of the above argument to equations other than (1) (and in particular to the case studied in sections 2 and 3) is straightforward. Only the form of the linear equation is changed and the only effect on the final result (7) is that one has to use a different function $v(\gamma)$.

When expression (7) is compared in figure 1 to the results of the simulations, the agreement is excellent. Moreover, in region II, one sees from (25) and (28) that

$$s_\varepsilon(z) \simeq \frac{A}{\pi \gamma_0} |\log \varepsilon| \sin\left(\frac{\pi \gamma_0 z}{|\log \varepsilon|}\right) e^{-\gamma_0 z}, \qquad (30)$$

which also agrees with the scaling form (20).

Recently, for a simple model of evolution [19, 20] governed by a linear equation, the velocity was found to be the logarithm of the cut-off to the power $\frac{1}{3}$. This result was obtained by an analysis which has some similarities to the one presented in this section.

5   A stochastic model

Many models described by traveling wave equations originate from a large scale limit of microscopic stochastic models involving a finite number N of particles [13, 14, 15, 16]. Here we study such a microscopic model, the limit of which reduces to (13) when $N \to \infty$. Our numerical results, presented below, indicate a large N correction to the velocity of the form $v_N \simeq v_0 - a (\log N)^{-2}$ with a coefficient a consistent with the one calculated in section 4 for $\varepsilon = \frac{1}{N}$.

The model we consider in this section appears in the study of directed polymers [14] and is, up to minor changes, equivalent to a model describing the dynamics of hard spheres [15]. It is a stochastic process discrete both in time and space with two parameters: N, the number of particles, and p, a real number between 0 and 1. At time t (t is an integer), we have N particles on a line at integer positions $x_1(t)$, $x_2(t)$, ..., $x_N(t)$. Several particles may occupy the same site. At each time-step, the N positions evolve in the following way: for each i, we choose two particles j_i and j_i' at random among the N particles. (These two particles do not need to be different.) Then we update $x_i(t)$ by

$$x_i(t+1) = \max\left(x_{j_i}(t) + \alpha_i,\, x_{j_i'}(t) + \alpha_i'\right), \qquad (31)$$

where α_i and α_i' are two independent random numbers taking the value 1 with probability p or 0 with probability $1 - p$. The numbers α_i, α_i', j_i and j_i' change at each time-step. Initially ($t = 0$), all particles are at the origin so that we have $x_i(0) = 0$ for all i.

At time t, the distribution of the $x_i(t)$ on the line can be represented by a function $h(x, t)$ which counts the fraction of particles strictly at the right of x.

$$h(x, t) = \frac{1}{N} \sum_{x_i(t) > x} 1. \qquad (32)$$

Obviously $h(x, t)$ is always an integral multiple of $\frac{1}{N}$. At $t = 0$, we have $h(x, 0) = 1$ if $x < 0$ and $h(x, 0) = 0$ if $x \geq 0$. One can notice that the definition of the position X_t of the front used in (11) coincides with

6

the average position of the N particles

$$X_t = \sum_{x=0}^{+\infty} h(x,t) = \frac{1}{N} \sum_{i=1}^{N} x_i(t). \qquad (33)$$

Given the positions $x_i(t)$ of all the particles (or, equivalently given the function $h(x,t)$), the $x_i(t+1)$ become independent random variables. Therefore, given $h(x,t)$, the probability for each particle to have at time $t+1$ a position strictly larger than x is given by

$$\langle h(x,t+1) \,|\, h(x,t) \rangle \qquad (34)$$
$$= 1 - \big[1 - ph(x-1,t) - (1-p)h(x,t)\big]^2.$$

The difficulty of the problem comes from the fact that one can only average $h(x,t+1)$ over a single time-step. On the right hand side of (34) we see terms like $h^2(x,t)$ or $h(x-1,t)h(x,t)$ and one has to calculate all the correlations of the $h(x,t)$ in order to find $\langle h(x,t+1) \rangle$. This makes the problem very difficult for finite N. However, given $h(x,t)$, the $x_i(t+1)$ are independent and in the limit $N \to \infty$, the fluctuations of $h(x,t+1)$ are negligible. Therefore, when $N \to \infty$, $h(x,t)$ evolves according to the deterministic equation (13). As the initial condition is a step function, we expect the front to move, in the limit $N \to \infty$, with the minimal velocity v_0 of (14).

For large but finite N, we expect the correction to the velocity to have two main origins. First, $h(x,t)$ takes only values which are integral multiples of $\frac{1}{N}$, so that $\frac{1}{N}$ plays a role similar to the cut-off ε of section 2. Second, $h(x,t)$ fluctuates around its average and this has the effect of adding noise to the evolution equation (13). In the rest of this section we present the results of simulations done for large but finite N and we will see that the shift in the velocity seems to be very close to the expression of section 4 when $\varepsilon = \frac{1}{N}$.

With the most direct way of simulating the model for N finite, it is difficult to study systems of size much larger than 10^6. Here we use a more sophisticated method allowing N to become huge. Our method, which handles many particles at the same time, consists in iterating directly $h(x,t)$.

Knowing the function $h(x,t)$ at time t, we want to calculate $h(x,t+1)$. We call respectively $x_{\min}$ and $x_{\max}$ the positions of the leftmost and rightmost particles at time t and $l = x_{\max} - x_{\min} + 1$. In terms of the function $h(x,t)$, one has $0 < h(x,t) < 1$ if and only if $x_{\min} \le x < x_{\max}$. Obviously, all the positions $x_i(t+1)$ will lie between $x_{\min}$ and $x_{\max} + 1$. The probability p_k that a given particle i will be located at position $x_{\min} + k$ at time $t+1$ is

$$p_k = \langle h(x_{\min} + k - 1, t+1) \rangle - \langle h(x_{\min} + k, t+1) \rangle, \qquad (35)$$

with $\langle h(x,t+1) \rangle$ given by (34). Obviously, $p_k \ne 0$ only for $0 \le k \le l$.

The probability to have, for every k, n_k particles at location $x_{\min} + k$ at time $t+1$ is given by

$$P(n_0, n_1, \dots, n_l) = \frac{N!}{n_0! \, n_1! \, \dots \, n_l!} \, p_0^{n_0} \, p_1^{n_1} \, \dots \, p_l^{n_l}$$
$$\times \, \delta(N - n_0 - n_1 - \dots - n_l). \qquad (36)$$

Using a random number generator for a binomial distribution, expression (36) allows to generate random n_k. This is done by calculating n_0 according to the distribution

$$P(n_0) = \frac{N!}{n_0! \, (N - n_0)!} \, p_0^{n_0} (1 - p_0)^{N - n_0}, \qquad (37)$$

then n_1 with

$$P(n_1 \,|\, n_0) = \frac{(N - n_0)!}{n_1! \, (N - n_0 - n_1)!} \left(\frac{p_1}{1 - p_0} \right)^{n_1}$$
$$\times \left(1 - \frac{p_1}{1 - p_0} \right)^{N - n_0 - n_1}, \qquad (38)$$

and so on. This method can be iterated to produce the $l+1$ numbers $n_0, n_1, \dots, n_l$ distributed according to (36). Then we construct $h(x,t+1)$ by

$$h(x,t+1) = 1 \qquad \text{if } x < x_{\min},$$
$$h(x,t+1) = \frac{1}{N} \sum_{i=k+1}^{l} n_i \qquad \begin{array}{l} \text{if } x_{\min} \le x \le x_{\max} + 1 \\ \text{and } x = x_{\min} + k, \end{array}$$
$$h(x,t+1) = 0 \qquad \text{if } x > x_{\max} + 1. \qquad (39)$$

As the width l of the front is roughly of order $\log N$, this method allows N to be very large.

Using this method with the generator of random binomial numbers given in [21], we have measured the velocity v_N of the front for several choices of p (0.05, 0.25 and 0.45) and for N ranging from 100 to 10^{16}. We measured the velocities with the expression

$$v_N = \frac{X_{10^6} - X_{10^5}}{9\,10^5}. \tag{40}$$

Figure 3 is a log-log plot of the difference $v_0 - v_N$ versus $\frac{1}{N}$ compared to the prediction (7) for $\varepsilon = \frac{1}{N}$. The variation of v_N when using longer times or different random numbers were not larger than the size of the symbols.
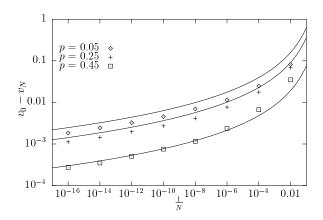

Figure 3: The difference $v_0 - v_N$ versus $\frac{1}{N}$ for three choices of p. The symbols represent the result of our numerical simulations of the stochastic process and the solid lines indicate the prediction (7) for $\varepsilon = \frac{1}{N}$.

We see on figure 3 that the speed v_N of the front seems to be given for large N by

$$v_N \simeq v_0 - \frac{K}{(\log N)^2}, \tag{41}$$

where the coefficient K is not too different from the prediction (7).

The agreement is however not perfect. The shift $v_0 - v_N$ seems to be proportional to $(\log N)^{-2}$, but the constant looks on figure 3 slightly different

from the one predicted by (7). A possible reason for this difference could have been the discretization of the front: instead of only cutting off the tail as in sections 3 and 4, here the whole front $h(x,t)$ is constrained to take values multiple of $\frac{1}{N}$. One might think that this could explain this discrepancy. However, we have checked numerically (the results are not presented in this paper) that equation (13) with $h(x,t)$ constrained to be a multiple of a cut-off ε does not give results significantly different from the simpler model of sections 3 and 4 with only a single cut-off. So we think that the full discretization of the front can not be responsible for a different constant K. The discrepancy observed in figure 3 is more likely due to the effect of the randomness of the process. It is however not clear whether this mismatch would decrease for even larger N. It would be interesting to push further the numerical simulations and check the N-dependence of the front velocity for very large N.

6   Conclusion

We have shown in the present work that a small cut-off ε in the tail of solutions of traveling wave equations has the effect of selecting a single velocity v_ε for the front. This velocity v_ε converges to the minimal velocity v_0 when $\varepsilon \to 0$ and the shift $v_0 - v_\varepsilon$ is surprisingly large (7, 8).

Very slow convergences to the minimal velocity have been observed in a number of cases [8, 13, 14, 15] as well as the example of section 5. As the effect of the cut-off on the velocity is large, it is reasonable to think that it would not be much affected by the presence of noise. The example of section 5 shows that the cut-off alone gives at least the right order of magnitude for the shift and it would certainly be interesting to push further the simulations for this particular model to see whether the analysis of section 4 should be modified by the noise. The numerical method used in section 5 to study a very large ($N \sim 10^{16}$) system was very helpful to observe a logarithmic behavior. We did not succeed to check in earlier works [13, 14, 15, 22] whether the correction was logarithmic, mostly because the published data

were usually too noisy or obtained on a too small range of the parameters. Still even if the cut-off was giving the main contribution to the shift of the velocity, other properties would remain very specific to the presence of noise like the diffusion of the position of the front [16].

Our approach of section 4 shows that the effect of a small cut-off is the existence of a scaling form (20, 30) which describes the change in the shape of the front in its steady state. The effect of initial conditions for usual traveling wave equations (with no cut-off) leads to a very similar scaling form for the change in the shape of the front in the transient regime. This is explained in the appendix where we show how the logarithmic shift of the position of a front due to initial conditions [10, 23] can be recovered.

A Effect of initial conditions on the position and on the shape of the front

In this appendix we show that ideas very similar to those developed in section 4 allow one to calculate the position and the shape at time t of a front evolving according to (1), or to a similar equation, given its initial shape. The main idea is that in the long time limit, there is a region of size $\sqrt{t}$ ahead of the front which keeps the memory of the initial condition. We will recover in particular the logarithmic shift in the position of the front due to the initial condition [10, 23], namely that if the initial shape is a step function

$$
\begin{array}{llll}
h(x,0) = & 0 & \text{if } x > 0, & \text{(A.1)} \\
h(x,0) = & 1 & \text{if } x < 0,
\end{array}
$$

then the position X_t of the front at time t increases like

$$
X_t \simeq 2t - \frac{3}{2} \log t. \qquad \text{(A.2)}
$$

More generally, if initially

$$
\begin{array}{llll}
h(x,0) = & x^\nu e^{-\gamma_0 x} & \text{if } x > 0, & \text{(A.3)} \\
h(x,0) = & 1 & \text{if } x < 0,
\end{array}
$$

we will show that for $\nu > -2$

$$
X_t \simeq 2t + \frac{\nu - 1}{2} \log t, \qquad \text{(A.4)}
$$

whereas the shift is given by (A.2) for $\nu < -2$. Here, there is no cut-off but the transient behavior in the long time limit gives rise to a scaling function very similar to the one discussed in section 4.

If we write the position of the front at time t as

$$
X_t = v_0 t - c(t), \qquad \text{(A.5)}
$$

we observed numerically (as in figure 2 of section 3) and we are going to see in the following that the shape of the front takes for large t the scaling form

$$
h(x,t) = t^\alpha G\left(\frac{x - X_t}{t^\alpha}\right) e^{-\gamma_0(x - X_t)}, \qquad \text{(A.6)}
$$

very similar to (20, 30).

If we use (A.5) and (A.6) into the linearized form of equation (1), we get using, the fact that $v_0 = 2$ and $\gamma_0 = 1$,

$$
\frac{1}{t^\alpha} G'' + \frac{1}{t^{1-\alpha}} \left(\alpha z G' - \alpha G\right) + t^\alpha \dot{c} G = \dot{c} G', \quad \text{(A.7)}
$$

where $z = (x - X_t) t^{-\alpha}$. By writing that the leading orders of the different terms of (A.7) are comparable, we see that we must have

$$
\alpha = \frac{1}{2}, \qquad \text{(A.8)}
$$

$$
\dot{c} \simeq \frac{\beta}{t}, \qquad \text{(A.9)}
$$

for some β, and that the right hand side of (A.7) is negligible. Therefore, the equation satisfied by G is

$$
\frac{d^2}{dz^2} G + \frac{z}{2} \frac{d}{dz} G + \left(\beta - \frac{1}{2}\right) G = 0, \qquad \text{(A.10)}
$$

and the position of the front is given by

$$
X_t \simeq v_0 t - \beta \log t. \qquad \text{(A.11)}
$$

As in section 4, we expect that as $t \to \infty$, the front will approach its limiting form and therefore that for z small, the shape will look like (15). Therefore we

9

choose the solution $G_\beta(z)$ of (A.10) which is linear at $z = 0$. This solution can be written as an infinite sum

$$G_\beta(z) = A \sum_{n=0}^{\infty} \frac{(-1)^n}{(2n+1)!} z^{2n+1} \prod_{i=0}^{n-1} (\beta + i),$$

$$= A \sum_{n=0}^{\infty} \frac{(-1)^n}{(2n+1)!} \frac{\Gamma(n+\beta)}{\Gamma(\beta)} z^{2n+1}. \quad \text{(A.12)}$$

(The second expression is not valid when β is a non-positive integer.)

To determine β, one can notice that the scaling form (A.6) has to match the initial condition when x is large and t of order 1. We thus need to calculate the asymptotic behavior of $G(z)$ when z is large.

For certain values of β, there exist closed expressions of the sum (A.12). For instance,

$$
\begin{aligned}
G_{-2}(z) &= A\left(z + \frac{z^3}{3} + \frac{z^5}{60}\right), \\
G_{\frac{7}{2}}(z) &= A\left(z - \frac{z^3}{3} + \frac{z^5}{60}\right) e^{-\frac{z^2}{4}}, \\
G_{-1}(z) &= A\left(z + \frac{z^3}{6}\right), \\
G_{\frac{5}{2}}(z) &= A\left(z - \frac{z^3}{6}\right) e^{-\frac{z^2}{4}}, \quad \text{(A.13)} \\
G_0(z) &= Az, \\
G_{\frac{3}{2}}(z) &= Aze^{-\frac{z^2}{4}}, \\
G_1(z) &= Ae^{-\frac{z^2}{4}} \int_0^z e^{\frac{t^2}{4}} dt, \\
G_{\frac{1}{2}}(z) &= A \int_0^z e^{-\frac{t^2}{4}} dt,
\end{aligned}
$$

One can check directly on (A.10) that G_β has a symmetry

$$G_\beta(z) = -ie^{-z^2/4} G_{\frac{3}{2}-\beta}(iz). \quad \text{(A.14)}$$

For any β, one can obtain the large z behavior of $G(z)$. To do so, we note that for $\beta > 0$, one can rewrite (A.12) as

$$
\begin{aligned}
G_\beta(z) &= \frac{A}{\Gamma(\beta)} \int_0^\infty dt\, t^{\beta-\frac{3}{2}} \sin(\sqrt{t}z)e^{-t}, \\
&= \frac{2A}{\Gamma(\beta)} z^{1-2\beta} \int_0^\infty dt\, t^{2\beta-2} \sin(t) e^{-\frac{t^2}{z^2}} \text{(A.15)}
\end{aligned}
$$

For $0 < \beta < 1$, the second integral in (A.15) has a non zero limit and this gives the asymptotic behavior of $G_\beta(z)$

$$G_\beta(z) \simeq -\frac{2A}{\Gamma(\beta)} \cos(\pi\beta)\,\Gamma(2\beta - 1)z^{1-2\beta}. \quad \text{(A.16)}$$

From (A.12), one can also show that

$$G''_\beta = -\frac{\Gamma(\beta+1)}{\Gamma(\beta)} G_{\beta+1}, \quad \text{(A.17)}$$

implying that (A.16) remains valid for all β except for $\beta = \frac{3}{2}, \frac{5}{2}, \frac{7}{2}$, etc., where the amplitude in (A.16) vanishes. For these values of β, $G_\beta(z)$ decreases faster than a power law (see (A.13)).

The functions G_β calculated so far are acceptable scaling functions for the shape of the front only for $\beta \leq \frac{3}{2}$. Indeed, one can see in (A.16) that for $\frac{3}{2} < \beta < \frac{5}{2}$ the function $G_\beta(z)$ is negative for large z. In fact, for all $\beta > \frac{3}{2}$, this function changes its sign at least once, so that the scaling form (A.6) is not reachable for an initial $h(x, 0)$ which is always positive. It is only for $\beta \leq \frac{3}{2}$ that G_β remains positive for all $z > 0$.

Looking at the asymptotic form (A.16), we see that if initially $h(x, 0) = x^\nu e^{-\gamma_0 x}$, the only function $G_\beta(z)$ which has the right large z behavior is such that $1 - 2\beta = \nu$, and this gives, together with (A.11), the expression (A.4) for the shift of the position. As the cases $\beta > \frac{3}{2}$ are not reachable, all initial conditions corresponding to $\nu < -2$ or steeper (such as step functions) give rise to $G_{\frac{3}{2}}$ and the shift in position given by (A.2).

All the analysis of this appendix can be extended to other traveling wave equations such as (13), with more general functions $v(\gamma)$ (having a non-degenerate minimum at γ_0) as in (14). Then the expressions (A.2, A.4) of the shift become

$$X_t \simeq v_0 t - \frac{3}{2\gamma_0} \log t \quad \text{(A.18)}$$

and

$$X_t \simeq v_0 t - \frac{1-\nu}{2\gamma_0} \log t. \quad \text{(A.19)}$$

10

References

[1] R. A. Fisher, "The Wave of Advance of Advantageous Genes," Annals of Eugenics **7,** 355–369 (1937).

[2] A. Kolmogorov, I. Petrovsky, and N. Piscounov, "Étude de l'Équation de la Diffusion avec Croissance de la Quantité de Matière et son Application à un Problème Biologique," Moscou Univ. Bull. Math. A **1,** 1 (1937).

[3] D. G. Aronson and H. F. Weinberger, "Multidimensional Nonlinear Diffusion Arising in Population Genetics," Advances in Mathematics **30,** 33–76 (1978).

[4] G. Dee and J. S. Langer, "Propagating Pattern Selection," Physical Review Letters **50,** 383–386 (1983).

[5] M. Bramson, P. Calderoni, A. D. Masi, P. Ferrari, J. L. Lebowitz, and R. H. Schonmann, "Microscopic Selection Principle for a Diffusion-Reaction Equation," Journal of Statistical Physics **45,** 905–920 (1986).

[6] W. van Saarloos, "Front Propagation into Unstable States. Linear Versus Nonlinear Marginal Stability and Rate of Convergence," Physical Review A **39,** 6367–6390 (1989).

[7] P. Collet and J.-P. Eckmann, *Instabilities and Fronts in Extended Systems* (Princeton University Press, 1990).

[8] A. R. Kerstein, "Computational Study of Propagating Fronts in a Lattice-Gas Model," Journal of Statistical Physics **45,** 921–931 (1986).

[9] D. G. Aronson and H. F. Weinberger, "Nonlinear Diffusion in Population Genetics, Combustion, and Nerve Propagation," Lecture Notes in Mathematics **446,** 5–49 (1975).

[10] M. Bramson, *Convergence of Solutions of the Kolmogorov Equation to Traveling Waves*, No. 285 in *Memoirs of the American Mathematical Society* (AMS, 1983).

[11] W. van Saarloos, "Dynamical Velocity Selection: Marginal Stability," Physical Review Letters **58,** 2571–2574 (1987).

[12] W. van Saarloos, "Front Propagation into Unstable States: Marginal Stability as a Dynamical Mechanism for Velocity Selection," Physical Review A **37,** 211–229 (1988).

[13] H. P. Breuer, W. Huber, and F. Petruccione, "Fluctuation Effects on Wave Propagation in a Reaction-Diffusion Process," Physica D **73,** 259–273 (1994).

[14] J. Cook and B. Derrida, "Lyapunov Exponents of Large, Sparse Random Matrices and the Problem of Directed Polymers with Complex Random Weights," Journal of Statistical Physics **61,** 961–986 (1990).

[15] R. van Zon, H. van Beijeren, and C. Dellago, "Largest Lyapunov Exponent for Many Particle Systems at Low Densities," Physical Review Letter **80,** 2035–2038 (1998).

[16] H. P. Breuer, W. Huber, and F. Petruccione, "The Macroscopic Limit in a Stochastic Reaction-Diffusion Process," Europhysics Letters **30,** 69–74 (1995).

[17] B. Derrida and H. Spohn, "Polymers on Disordered Trees, Spin Glasses, and Traveling Waves," Journal of Statistical Physics **51,** 817–840 (1988).

[18] B. Derrida, "Mean field theory of directed polymers in a random medium," Physica Scripta **38,** 6–12 (1991).

[19] D. A. Kessler, H. Levine, D. Ridgway, and L. Tsimring, "Evolution on a Smooth Landscape," Journal of Statistical Physics **87,** 519–544 (1997).

[20] L. Tsimring, H. Levine, and D. A. Kessler, "RNA Virus Evolution via a Fitness-Space Model," Physical Review Letters **76,** 4440–4443 (1996).

[21] W. H. Press, S. A. Teukolsky, W. T. Vetter-
ling, and B. P. Flannery, *Numerical Recipes in
C* (Cambridge University Press, 1994).

[22] A. R. Kerstein, "A Two-Particle Representation
of Front Propagation in Diffusion-Reaction Sys-
tems," Journal of Statistical Physics **53,** 703–
712 (1988).

[23] M. D. Bramson, "Maximal Displacement of
Branching Brownian motion," Communications
In Pure and Applied Mathematics **31,** 531–581
(1978).